Numerical Model Studies of the Winter-Storm Response of the West Florida Shelf

YA HSUEH, G. O. MARMORINO AND LINDA L. VANSANT

Department of Oceanography, Florida State University, Tallahassee 32306

(Manuscript received 2 February 1982, in final form 1 July 1982)

ABSTRACT

The wintertime, wind-driven ocean circulation on the West Florida Continental Shelf is studied within the framework of a linearized storm-surge model. The model bathymetry incorporates a realistic shelf, extending from New Orleans to the southern tip of Florida, and a deep ocean region. The boundary condition at the coast is that there is no normal flow. At the open boundaries, located off the shelf in deep water, the adjusted sea level is fixed at zero.

It is found that 1) a coastally trapped response is achieved within one local inertial period following the imposition of the wind; 2) the curved coast forces a mass exchange between the coastal water and the deep ocean; 3) this exchange leads to the generation of a series of mesoscale eddies along the shelf edge; and 4) these eddies give rise to long-period, shelf-wide oscillations that persist beyond the local spin-up time.

A hindcast of the wind-driven flow on the West Florida Shelf for a particular period (11–25 March 1978) that contains the passage of a distinct cold front produces coastal sea-level and current fluctuations that are in reasonable agreement with observations.

1. Introduction

The West Florida Continental Shelf (Fig. 1) is a vast semienclosed area, the 100 m isobath often lying 200 km offshore along its 1000 km path from the Florida Straits in the south to the constricted areas in the northwest off the Mississippi Delta. In the winter, under the influence of frequent outbreaks of cold continental air from the north, the inner-shelf water becomes vertically well mixed and isolated from the open-ocean processes farther offshore. This paper addresses the time-dependent sea level and velocity response of the shelf under such conditions.

The few direct current measurements on the shelf in winter have shown (Price and Mooers, 1974; Mitchum and Sturges, 1981) a strong wind-driven response inside the 50 m isobath. Statistical studies of coastal sea level also show (Cragg *et al.*, 1981; Marmorino, 1982) a straightforward wind-driven response. Coastal sea levels are found to lag the wind by generally less than a day with some evidence for a dependence upon storm path. Efforts to detect propagating disturbances such as shelf waves have been hampered so far because of the overwhelming wind-driven coastal sea-level signal and the lack of any alongshore separation in the current meter moorings. Under the limitations of steady-state Ekman dynamics with linear bottom friction, some of the spatial variability in the response can be reproduced [Marmorino (1982)]. For example, under the influence of southeastward (essentially alongshore) wind stress, alongshore sea-levels are set-down, minimum values occurring in the bight between Clearwater and Apalachicola. Marmorino's (1982) model domain stopped at Panama City, so that even the steady-state response beyond that is unexplored.

To extend the previous studies, a time-dependent model (described in Section 2) is used to explore the transient response of the entire shelf to atmospheric forcing of both a hypothetical (impulsively begun experiments are described in Section 3; response to idealized moving fronts in Section 4) and realistic (a hindcast of a 1978 winter storm in Section 5) nature. Questions that could not be dealt with fully in the earlier work will be studied further here by investigation of 1) the time scales over which the flow is brought into frictional adjustment with the forcing; 2) the important force balances and how they change along the shelf; 3) whether any circulation cells are induced by the major change in coastline orientation; and 4) the possible role of free-wave propagation during the relaxation phase that follows forcing events.

2. The numerical model

Since interest is in the barotropic response, the model equations are taken to be the depth-integrated, linearized, shallow-water equations:

$$U_t - fV = -gh(\eta + \eta_a)_x + \tau_s^{(x)} - \tau_b^{(x)}, \quad (1)$$

$$V_t + fU = -gh(\eta + \eta_a)_y + \tau_s^{(y)} - \tau_b^{(y)}, \quad (2)$$

$$U_x + V_y = -\eta_t\,. \quad (3)$$

Here, U and V are the x and y transports; f, the Coriolis parameter set equal to a constant [6.62

0022-3670/82/101037-14$07.50

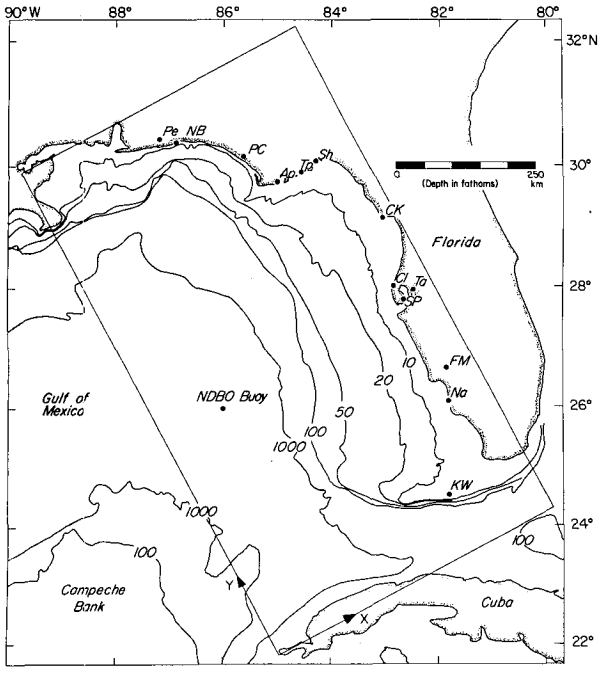

FIG. 1. Eastern Gulf of Mexico (depths in fathoms), traced from National Ocean Survey Chart 411. The rectangle is the model domain (see Fig. 2). Tide-gauge stations are Pe (Pensacola), NB (Navarre Beach), PC (Panama City), AP (Apalachicola), Tp (Turkey Point, Florida State University Marine Laboratory), Sh (Shell Point), CK (Cedar Key), Cl (Clearwater), SP (St. Petersburg), FM (Fort Meyers), Na (Naples), KW (Key West). Meteorological stations are Pe, Ap, Ta (Tampa), FM, KW, and NOAA Data Buoy Office Buoy 42003.

$\times 10^{-5}$ s^{-1} (corresponding to 27.0°N)]; g, gravitational acceleration; h, the still-water depth; η, the elevation of the free surface above the still-water level; η_a, the atmospheric pressure divided by ρg; $\tau_s = \tau_s^{(x)}\hat{\mathbf{i}} + \tau_s^{(y)}\hat{\mathbf{j}}$, the kinematic surface wind stress; and $\tau_b = \tau_b^{(x)}\hat{\mathbf{i}} + \tau_b^{(y)}\hat{\mathbf{j}}$, the kinematic bottom stress, given by either a quadratic formula, $\tau_b = C_D\mathbf{U}|\mathbf{U}|h^{-2}$, or by a linear formula, $\tau_b = r\mathbf{U}h^{-1}$, where $\mathbf{U}$ is the transport vector, C_D the drag coefficient, and r the resistance coefficient.

The coastal boundary condition is that there is no normal flow. Elsewhere, along open boundaries, it is required that the adjusted sea level ($\eta + \eta_a$) be zero; as discussed by Beardsley and Haidvogel (1981), this isolates the shelf from open-ocean forcing processes making, in effect, the open ocean "inert." Over deep water, the assumption of constant adjusted sea level for the study of synoptic band disturbances seems a reasonable one as the ocean responds approximately in the manner of an inverted barometer (see, e.g., Brown *et al.*, 1975). It is where the open boundary lies over the shelf that inaccuracies may develop; hence the model domain was chosen to minimize these areas. Fig. 2 shows the domain in detail. The grid has a uniform spacing of 27.6 km and, at its largest, is 22 grid lines wide (i-direction) by 38 grid lines (j-direction). The potentially troublesome open boundaries lie along $i = 22$, where the shelf comes to a naturally abrupt end, and along $i = 1$, where the shelf has narrowed to the extent that the first offshore point (where $\eta + \eta_a = 0$) is near the shelf break.

The model bathymetry was created as follows: barrier islands and small-scale coastal inlets were ignored; shallow areas beyond the shelf to the south, judged to be of no significance to the shelf problem, were replaced with a smooth extension of the deep-water isobaths (cf. Figs. 1 and 2); the depth at the coast was arbitrarily set to 1 m to avoid division by zero in the model code and to be consistent with the linearization of the governing equations; and the topography associated with DeSoto Canyon (off-shore of Pensacola) was replaced with more smoothly varying isobaths, creating an especially simple bathymetry in the region of the first open boundary value at $(i, j) = (1, 33)$. The resulting bathymetry is a reasonable approximation to the West Florida Shelf; future modeling studies with greater spatial resolution can, perhaps, include some of the depth variability lacking in this effort. In the calculations, depths are further averaged; for Eq. (1), the average h in the y-direction is used; for Eq. (2), the x-average is used. In the later presentations of the transport neld, V's are averaged and combined with U to provide a U at U-points in the grid. (See Fig. 3 for the model stencil.) Values of

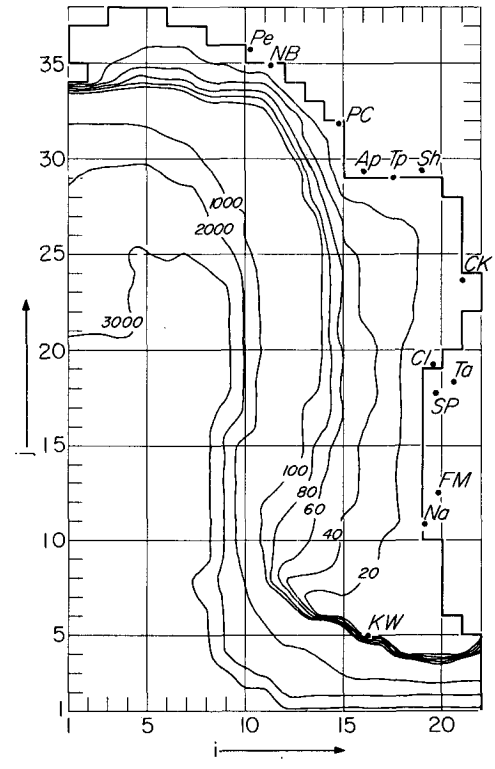

FIG. 2. Model bathymetry (depths in meters) and coordinate grid for the depth field. Grid interval is 27.6 km.

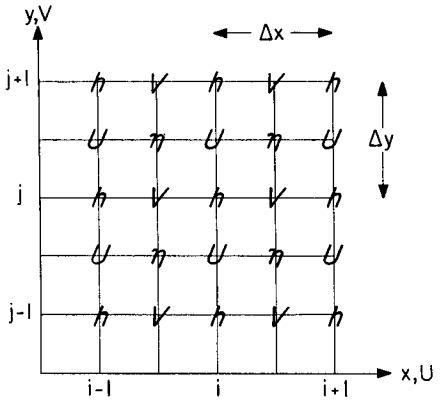

FIG. 3. The model (staggered-grid) stencil. Separation between values of any given variable is Δx or Δy. Values of wind stress are specified at h points; values of atmospheric pressure, at η points.

η associated with an open boundary and variables outside these η-points are not computed.

The computations follow the alternating-direction, semi-implicit scheme of Leendertse (1967). A spatially staggered grid (Fig. 3) and finite differences centered in space and forward in time are used. The model code is essentially the same as used by Vansant (1980) in a study of tidal-driven flow in Apalachicola Bay (see Fig. 1). Leendertse's (1967) algorithm (with nonlinear terms) was also used recently by Bowman *et al.* (1980). Based on the maximum model depth of 3294 m (1800 fathoms), the Courant-Friedrichs-Levy condition for a constant-depth basin is that the model time step, $\Delta t \leq (2^{1/2}/2)\Delta x/(gh)^{1/2} = 109$ s. Leendertse has shown, however, that his scheme is stable and accurate for Δt that exceed the CFL value. After checking that runs with $\Delta t = 100$ s and $\Delta t = 200$ s gave identical results, all further calculations used (the more economical value) $\Delta t = 200$ s.

All results reported here are for a linear bottom stress law with $r = 0.030$ cm s^{-1} (see Section 5). Computationally, there is no problem using the quadratic formulation but, physically, this is correct only when applied to the instantaneous velocities. On the West Florida Shelf, the instantaneous current has a large tidal component: for example, Mitchum and Sturges (1981) show that, on the 22 m isobath, the strongest alongshore synoptic flows are less than 30 cm s^{-1}, while the speed of the dominant M_2 tide is about 20 cm s^{-1} (rms). So, unless tidal currents are explicitly incorporated into the model, use of the more realistic quadratic law with a reasonable drag coefficient will not give correct answers. [An example of this more realistic approach is given by the work of Bowman *et al.* (1980), but, in their case, the regime was dominated by strong tides so that even a strong wind forcing had little effect on the answer.] Since the linear resistance coefficient parameterizes the effects of tidal and other high-frequency currents it provides a reasonable alternative at this stage at least.

3. Impulsive uniform stress experiments

In a fashion analogous to that of Beardsley and Haidvogel (1981), several initial-value experiments, in which a spatially uniform wind stress (held constant at 1 dyn cm^{-2}) is applied at $t = 0$ to an initially quiescent fluid, were run (for 7 days) to explore the adjustment of the shelf to sudden changes in forcing. Results for two experiments in which a unit stress is applied in either the negative y or negative x directions clearly show (Figs. 4–11) the sensitivity of the response to the orientation of the wind stress.

For a negative y (southeastward) directed wind stress, the response in the first few hours when rotational effects are insignificant is a set-down of sea level where the wind blows offshore and a set-up where the wind blows onshore. A remnant of this kind of response is still apparent in the sea-level field near Clearwater at 3 h (Fig. 4a). For longer times, sea level is depressed over the entire shelf, amplitudes increasing in the positive y (alongshore) direction. The zero-sea-level contour emanates from the shelf break near Key West and lies along the continental slope (well inside of the open-ocean $\eta = 0$ boundary), eventually extending from one corner of the domain to the other in the form of a series of positive (high sea level) eddies that slowly drift along the slope toward the northwest. Though the eddies do change shape (sometimes by coalescing), they maintain a size on the order of 2–4 grid intervals (50–100 km), being generally elongated in the cross-slope direction. On the shelf, the basic sea-level distribution is seen to be attained rather quickly (in about 1 day) and to change little afterward. A true steady-state solution is not obtained, however, because of the interaction between the shelf structure and the deep-water eddies (see later).

The propagation characteristics of the eddies is more clearly seen in Fig. 5 where sea level is contoured in y–t space along a fixed value of x (or i). Along $i = 10$, corresponding for the most part to the 1000 m isobath, lines of constant phase (the zero contour) tilt upward to the right for $j \leq 31$ implying phase propagation along the slope in the correct sense for a vorticity wave. The period of the wave is seen to be about 1.3 days, as measured at $j \approx 18$; from Fig. 4a, the along-slope wavelength is $\sim$110 km (4 grid intervals): thus, a phase speed of about 85 km day^{-1} is calculated. Note, however, that the phase speed at a fixed location decreases with time. On the shelf, along the 20 m isobath ($i = 18$), a fairly steady pattern is established after an adjustment period of about a day (see also Fig. 6). At the southern end of the shelf, amplitudes build up quickly (in less than a day), but oscillations with periods of $\sim$11 h persist for several days (Figs. 5 and 6); for large y, the influence of the offshore eddies superimposes a small-amplitude long-period oscillation.

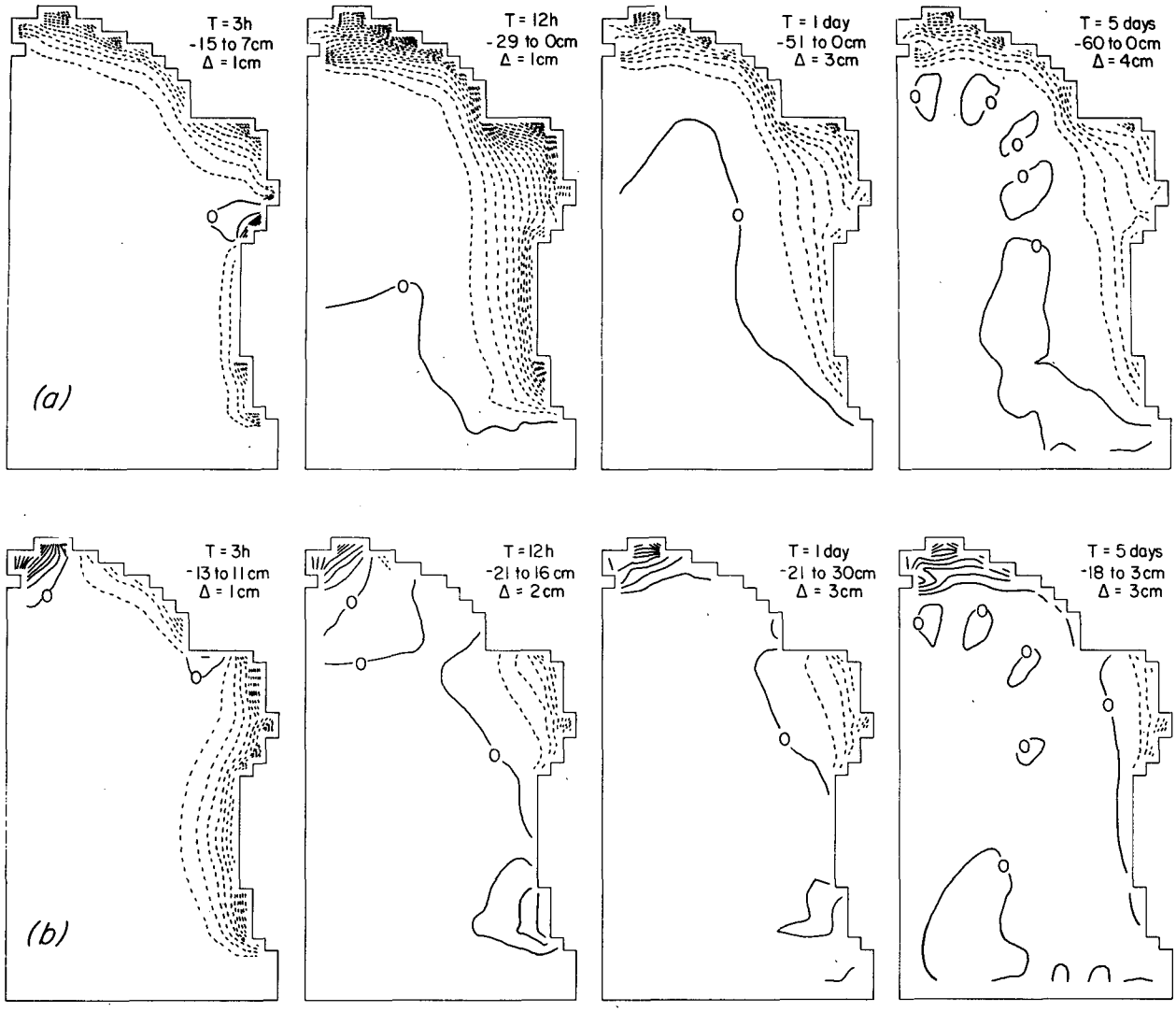

FIG. 4. Sea-level contours at t = 3 h, 12 h, 1 day and 5 days for a uniform unit wind stress impulsively applied in the (a) negative y direction and (b) negative x direction. The bottom resistance coefficient r is 0.030 cm s^{-1}. Minimum and maximum values and the contour interval Δ are given. Because the problem is linear, solutions for stresses in the positive directions are simply negatives of values shown.

In the $-x$ directed experiment, the response is weaker, being confined to a set-down in the Bight and a set-up off Pensacola (Fig. 4b). Again, eddies, somewhat less intense than before, drift along the slope. In this case, oscillations are excited throughout the shelf, increasing in period from again 11 h in the south to about 15 h in the Bight (Fig. 6). The amplitudes of the 11 h oscillations are largest in the semi-enclosed shallow region between Key West and Naples (i = 19, 6 < j < 10). Use of a seiche formula (Wilson, 1972) appropriate to this wedge-shaped region does yield a period of about 11 h. Again, the frictional adjustment time is about 1 day or so.

The along-coast distribution of sea level after 5 days for the impulsive experiments again demonstrates (Fig. 7) the much larger response in the case of the $-y$ directed stress. Fig. 7 also compares these results with steady-state distributions calculated with Hsueh's (1980) vorticity-equation model as used by Marmorino (1982). There, the similarly-oriented model domain begins at Key West and extends to about Panama City, the spatial resolution being about three times finer than in the present primitive-equation model. The dynamics (including linear bottom friction) is identical with the one exception that in the vorticity model, only the local alongshore component of the wind stress enters into the calculation. The basic behavior in the $-y$ directed case is the same in both calculations: a sea level response that grows in the y direction, emanating from the beginning of shelf (near Key West), largest amplitudes being found in the Bight, beyond which they decrease; in the prim-

itive-equation model, sea level response is largest in the shallow area beyond Pensacola. Agreement is not so good for the $-x$ directed case. There, the primitive-equation model lacks the finestructure off the Naples–Fort Meyers area made possible by the finer resolution of the vorticity model; the vorticity model underestimates the response in the Bight where the wind stress is locally offshore.

The mass transport fields after 12 h for the two impulsive experiments are compared in Fig. 8. Far from shore, in deep water, Ekman drift to the right of wind stress prevails; in both cases, this is about equal to the theoretical value $\tau_s/\rho f = 1.5 \times 10^4$ cm^2 s^{-1}. The $-y$ directed stress drives strong flow downwind with depth-averaged y-component currents of about 10 cm s^{-1} (see Figs. 9 and 10). This flow is forced to cross the steep shelf-break near Key West, stretching fluid columns and producing the vorticity waves seen previously. Notice that the Ekman drift offshore of the shelf is supplied by the wind-driven flow on the shelf (cf. Csanady, 1978). Large transports

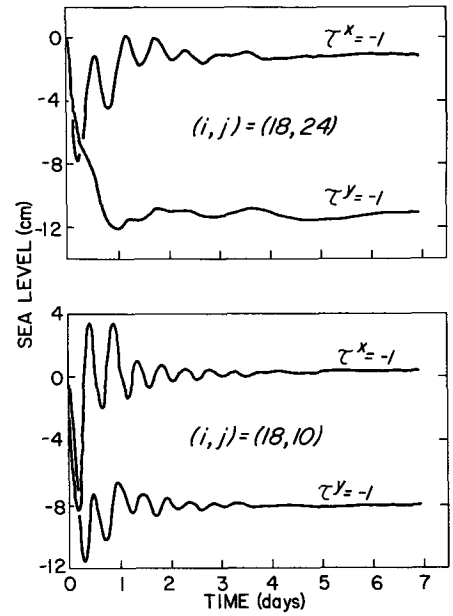

FIG. 6. Sea level time series for the impulsive stress experiments: (top) off Cedar Key, in about 21 m of water; (bottom) off Naples, 10 m.

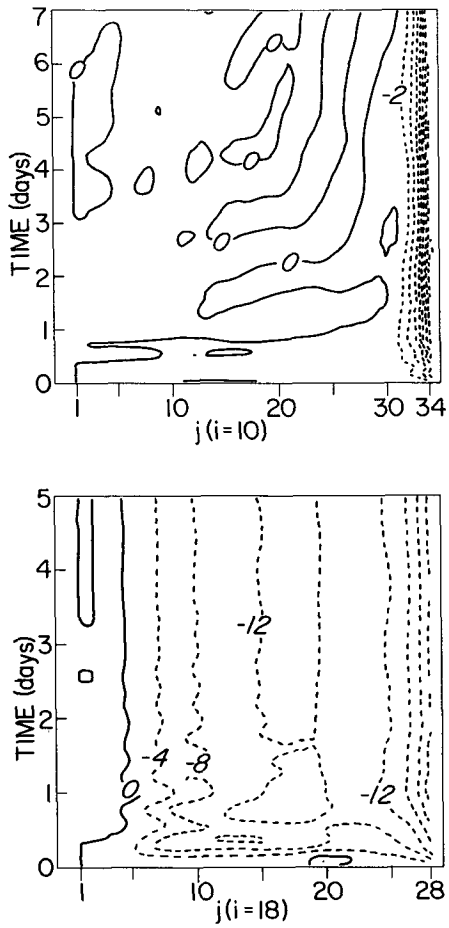

FIG. 5. Sea level contours in y–t space for the case of an impulsive stress in the negative y direction: (top) i = 10, along the slope; (bottom) i = 18, on the shelf.

(but small depth-averaged velocities) in the neighborhood of the northwest open boundary arise on account of the large pressure gradient between the imposed zero-sea-level condition along the boundary

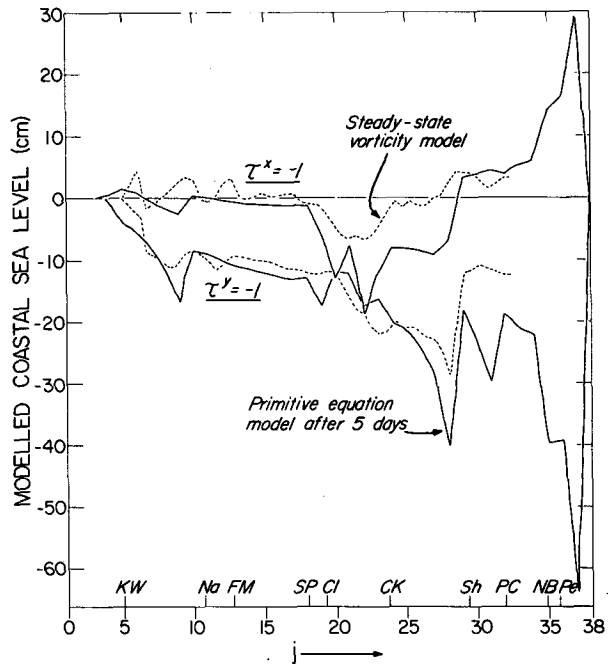

FIG. 7. Comparison of the impulsive stress experiments of this paper with the steady-state vorticity model (see Marmorino, 1982). In both calculations, r = 0.030 cm s^{-1}. The steady-state model has a finer spatial resolution but a smaller domain.

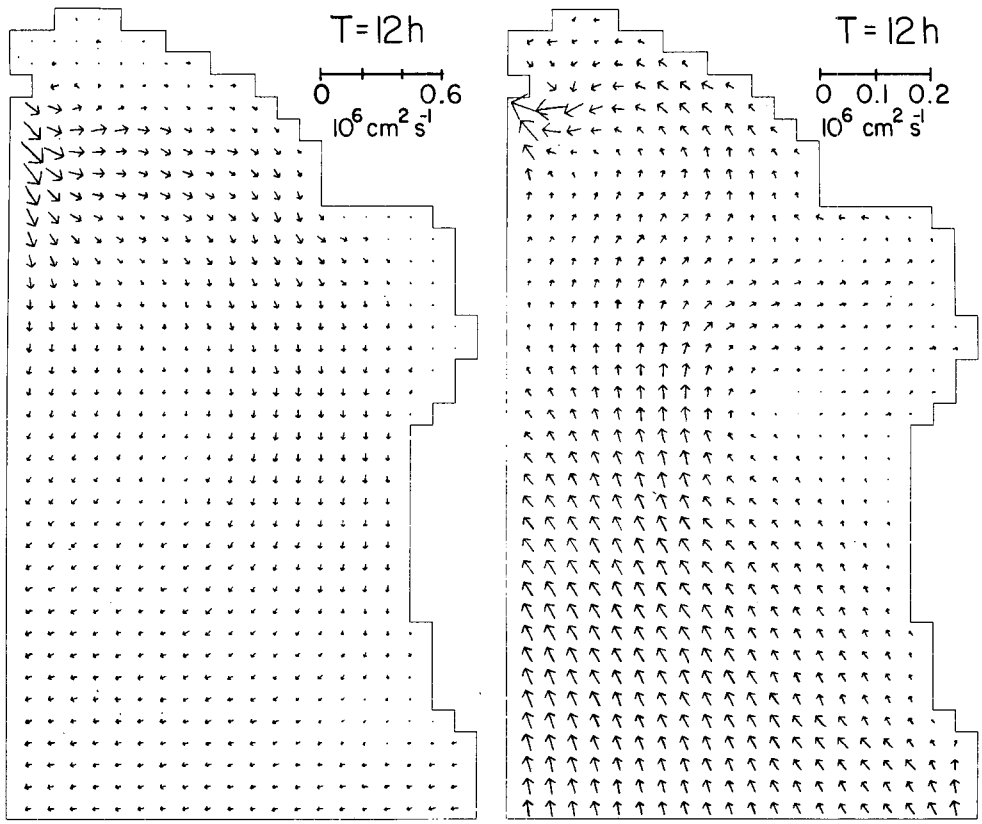

FIG. 8. Mass transport fields at 12 h for the impulsive stress experiments: left, the case of a stress in the negative y direction; right, negative x direction.

and the large negative sea-level values off the modeled coasts of Mississippi and Alabama. Part of this transport feeds the West Florida Shelf flow; part, the deep-ocean flow field. At later times (not shown), anticyclonic eddies (associated with the positive perturbations in sea level seen in Fig. 4a) perturb the simple pattern portrayed here. In the $-x$ directed case, the flow is generally weaker. Interestingly, offshore Ekman drift turns, supplying onshore flow directly into the Bight. In this case, depth-averaged flow in the *positive* y direction generates vorticity at the shelf-break near Key West; thus, after 5 days (Fig. 4b), *negative* sea-level perturbations with associated cyclonic flow are present in about the same locations as the positive eddies in the $-y$ stress experiment (Fig. 4a).

The time history, during the $-y$ stress experiment, of the cross-shelf structure of sea level and depth-averaged alongshore flow ($v = V/h$) is examined along two transects ($j = 23$ and $j = 15$) that are normal to the isobaths (Figs. 9 and 10). In both cases, there is an overshoot of the equilibrium ($t > 2$ days) solution (see also Fig. 6). The adjustment time is shorter along $j = 15$ than it is farther north at $j = 23$. Off Cedar Key (Fig. 9), the amplitudes decay to less than 5% of their coastal values at a distance of about 10 grid intervals from the coast (about 280 km), corresponding to a water depth of about 400 m. Since the mid-shelf sea level gradient is nearly constant at 9×10^{-7} (Fig. 9b), the geostrophic mid-shelf v should be about 13.4 cm s^{-1}, about what Fig. 9a shows. Very near-shore along $j = 23$, a small positive flow develops. Along $j = 15$ where the coastline is straighter, the signals decay exponentially offshore (in the manner of a coastal jet), reaching the 5% level at the 150 m isobath, 200 km offshore. (For comparison, the barotropic Rossby radius of deformation, representing the e-folding offshore scale, is at least 300 km.)

The predominance of geostrophy in the model longshore flow is unmistakable. A time-series plot for the $-y$ stress experiment of the balance of terms in the momentum equation at two grid points, each representative of a particular stretch of the coastal region, leaves little doubt that the cross-shelf gradient in sea level and the Coriolis term (fV) cancel (Fig. 11). Near the straight coast to the south [$(i, j) = (18, 15)$], this cancellation is achieved within a few hours of the imposition of the wind stress; in the y-momentum equation, near-equilibrium is struck between the source (wind stress) and sink (bottom friction) within one day of the start of the forcing. Within the Bight (19, 23), the x-momentum balance remains primarily geostrophic, although a small but noticeable amount of frictional loss is now present. The presence of τ_b

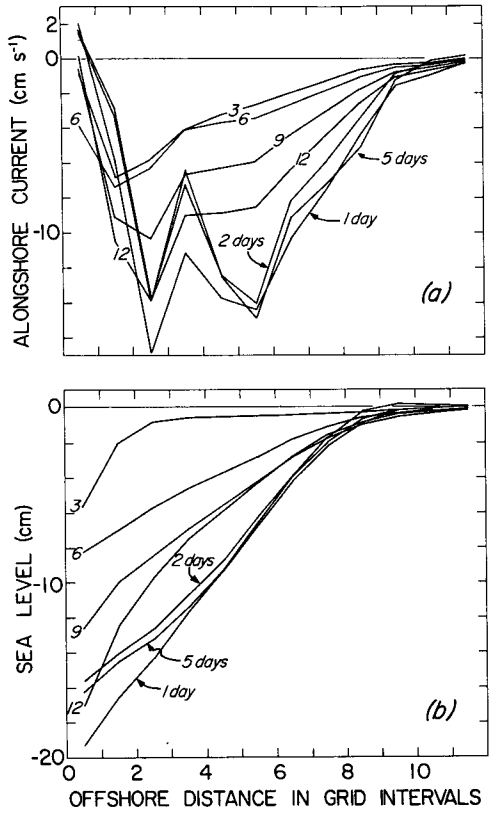

FIG. 9. Time evolution of cross-shelf structure along $j = 23$ for the $-y$ stress experiment. The numbers on the curve are in hours unless noted otherwise.

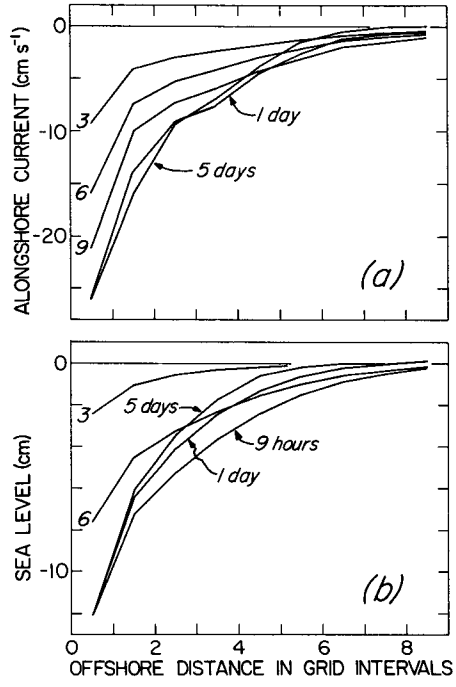

FIG. 10. Time evolution of cross-shelf structure along $j = 15$ for the $-y$ stress experiment. The numbers on the curve are in hours unless noted otherwise.

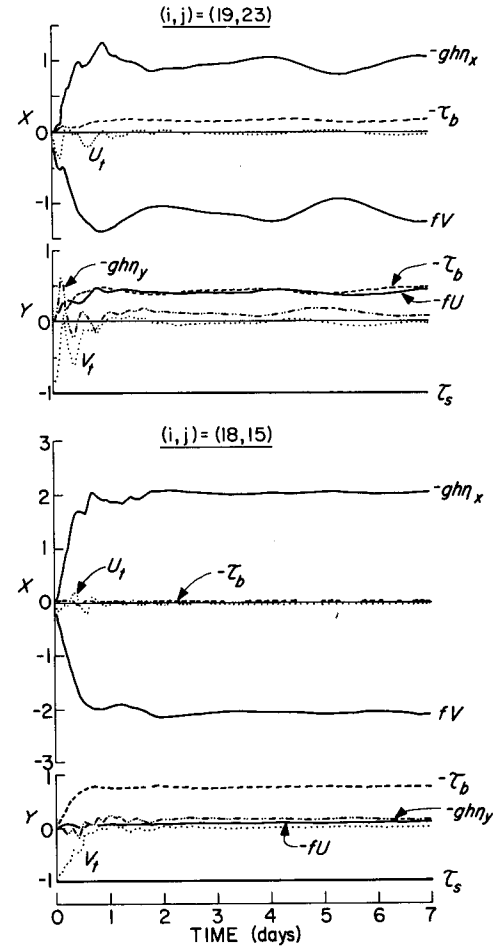

FIG. 11. Time history of terms in the X and Y momentum equations at two nearshore locations. Units are $cm^2\ s^{-1}$.

here is due to an enhancement in cross-shelf flow brought about by the indentation in the coastline around the Bight. The enhanced cross-shelf flow gives rise to a Coriolis term ($-fU$) that acts to redistribute the y momentum. The important consequence of this redistribution is that the local frictional loss now accounts for only less than half of the y momentum input from the wind. A simple source-sink type of y momentum balance has been used as the basis for estimating, from simultaneous observations of winds and currents, the bottom resistance coefficient (r) in a linear law of friction (Scott and Csanady, 1976; Mitchum and Sturges, 1981). It seems that the validity of such a balance may depend upon local features of circulation that can vary from point to point. This variation will be a source of uncertainty in the estimate of r.

4. An ideal cold front

A particularly frequent and energetic wind event over the West Florida Shelf in winter is the passage of a cold front. The principal features relating to the

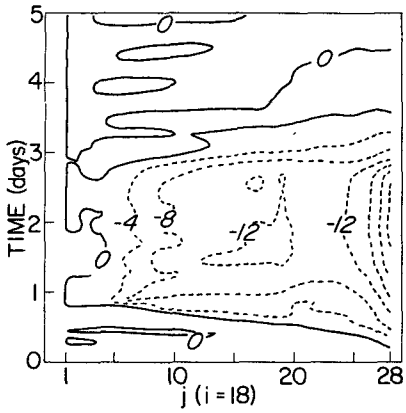

FIG. 12. Sea-level contours in y–t space along $i = 18$ for the case of wind stress forcing in the form of an idealized cold front.

wind as a forcing function during such an event are seen to be a period of frontal influence of ~4 days; a surface pressure that is lowest at the front; and winds that are northeastward in advance of the front, then rotate clockwise, becoming strong southeastward. Furthermore, the front translation speed is 8–12 m s^{-1} in winter; the frontal width is about 140 km; the atmospheric variables tend to be invariant along a direction parallel to the front; and the frontal characteristics are essentially preserved in the direction normal to the front as it moves in a generally southeastward direction (see Fernandez-Partagas and Mooers, 1975).

To understand the ocean response on the West Florida Shelf to such an event, a model experiment with a wind-stress pattern constructed in accordance with the above set of features was conducted. The pattern is composed of a field of $-y$ directed wind stress vectors that is invariant in the x direction. The wind-stress amplitude increases from zero in advance of the front to a uniform 1 dyn cm^{-2} behind. The width of the transition is 110 km (4 model grid intervals). The pattern advances in the $-y$ direction at a speed of 12.25 m s^{-1}. Thus the y wind stress over the entire model area becomes a constant -1 dyn cm^{-2} within about 20 h of the arrival of the forward edge of the front at the northwestern end. Two-and-a-half days into the experiment, the wind stress field is allowed to collapse to zero in 8 h. The model ocean is then left free of forcing for two more days before the experiment is terminated.

The results of the experiment are summarized in a y–t plot of the sea-level fluctuations along $i = 18$ (Fig. 12). Here, the coast is encountered at $j = 28$ where a zero contour emanates that bounds the front-forced response of a depression in sea level and slopes in accordance with the movement of the front in the $-y$ direction. After the front passes, a near steady state sets in (cf. Fig. 5, bottom) in which the sea-level depression increases in the y direction and reaches a maximum drop of 24 cm at $j = 28$. Note that, compared to the time of local front passage, nearly steady values are reached faster in the south (at low j values) than in the north (at larger j values), resembling Marmorino's (1982) observation that response times tend to decrease in the direction of front passage. On day 3, the forcing ceases and the zero-contour indicates free-wave propagation at a speed of ~500 km day^{-1}, a not unreasonable value for shelf waves. Closed loops of zero-sea-level contours that

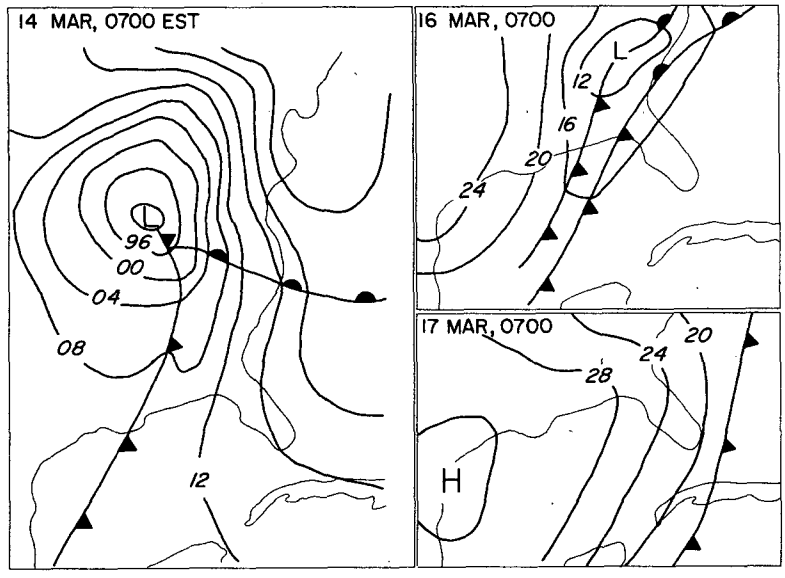

FIG. 13. Weather maps showing movement of cold front through the model domain during the period of the model hindcast.

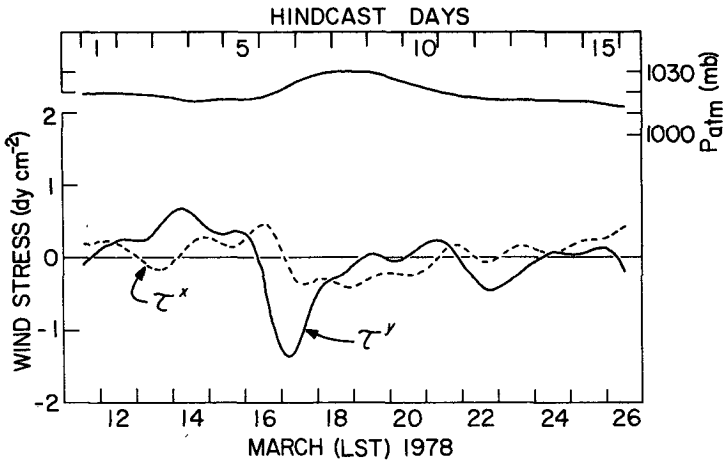

FIG. 14. Tampa wind-stress and atmospheric-pressure time series for the hindcast period.

move up the coast at 140 km day^{-1} may be higher wavenumber manifestations of the same species.

5. Hindcast

The numerical experiments so far described are hypothetical in nature. They are intended to expose the predominant characteristics of some distinct flow features that may be relevant to the winter-storm response of the West Florida Shelf. To establish the extent to which the model is indeed realistic, a hindcast is necessary in which the model is forced with observed winds and model outputs checked against observations. Coastal tide-gauge and meteorological records in the model area (see Fig. 1) for the period of January through April 1978 have been examined closely for low-frequency (periods >2 days) fluctuations by Marmorino (1982). Figs. 2 and 3 of Marmorino (1982) show the low-passed sea level and wind-stress components along the model coordinate axes at all available stations for the entire 1978 winter. A 14-day stretch during this period, Julian Day 70–84 (11–25 March), was chosen for the hindcast. This time span is marked by the passage of a cold front that is preceded by a warm front and followed by several days of relatively low winds. The movement of the synoptic weather pattern corroborates the frontal passage (Fig. 13). Upon trailing behind a warm

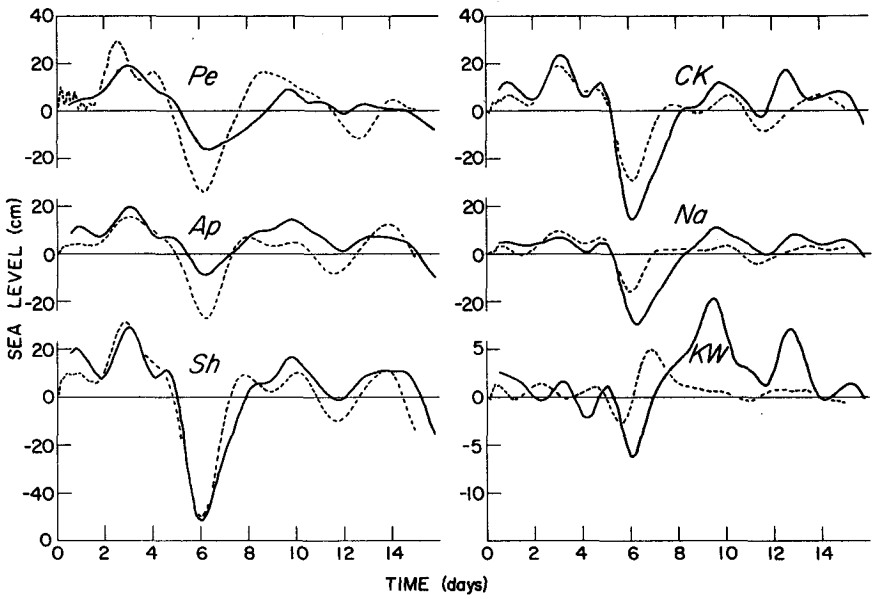

FIG. 15. Comparisons between observed and modeled sea-level fluctuations. Observed values have been adjusted for atmospheric pressure and have been mean-determined. Note the change in scale for Key West.

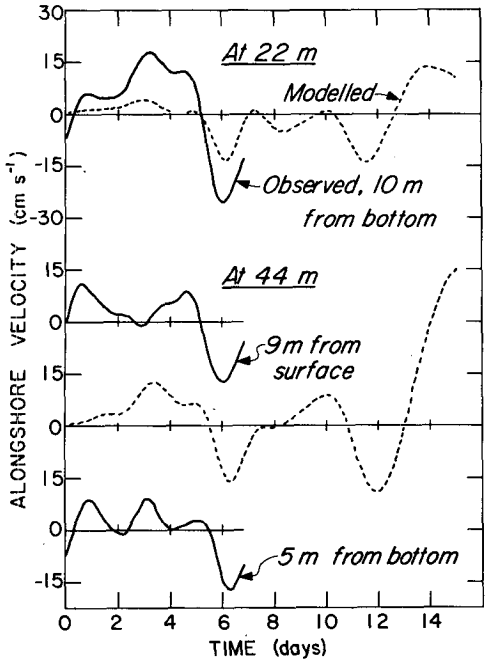

FIG. 16. Comparisons between observed and modeled y-directed velocities off Cedar Key. Model coordinates are (18, 23) and (16, 23) for the 22 and 44 m comparisons, respectively. At the 22 m mooring, a second record at 5 m from the bottom (not shown) is quite similar to the 10 m record. (Observed data courtesy of G. Mitchum and T. Sturges.)

front, the cold front made its approach on 14 March. It began the sweep on 16 March and crossed the entire West Florida Shelf in approximately one day.

The surface winds are used to create records of wind stress through the usual quadratic law with a drag coefficient of 1.5×10^{-3}. Low-passed wind-stress records are then decimated to provide a 6 h forcing over longshore bands of the shelf area. The Pensacola wind stress is applied from $j = 33$ to 38; the wind stress at Apalachicola is applied from $j = 24$ to 32; that at Tampa to $j = 16$ to 23; that at Fort Meyers to $j = 9$ to 15; and the Key West wind-stress forcing covers the rest of the shelf area. The wind stress in each band is uniform across the shelf (in the x direction) and is non-uniform in the y direction only to the extent that a Hanning smoothing is applied along the two adjoining grid lines between the bands. In applying coastal wind-stress values over the ocean, a major concern is the extent to which these values are representative of the open-water conditions. Comparison with values derived from observations at NOAA Data Buoy Office Buoy 42003, which was located 420 km from Tampa, indicates a three-fold overwater increase in wind stress (Marmorino, 1982). To account partially for this increase, the wind stresses at the coastal stations (but not at Key West) are doubled before being entered as inputs to the model. A two-fold increase in overwater surface winds is not unreasonable for the coastal wind magnitudes of 6–8 m s^{-1} encountered in the hindcast period (Hsu, 1981). To be consistent, the bottom resistance coefficient r (=0.03 cm s^{-1}) has also been set at about twice that found from observations on the basis of a purely source-sink momentum balance (Mitchum and Sturges, 1981). An example of the wind-stress time series used to drive the model is given by that at Tampa (Fig. 14). The upper curve represents the atmospheric pressure, which is not used in the model. Numerical experiment results (not shown) of atmospheric pressure-gradient forcing indicate that the amplitude of the non-barometric coastal sea-level response in this case is only a small fraction of that due to wind stress. This is, of course, quite in keeping with theoretical estimates (Gill and Schumann, 1974).

Model results are compared (Fig. 15) with low-passed sea-level records from Pensacola, Apalachicola, Shell Point, Cedar Key, Naples and Key West, from which the static response to atmospheric pressure has been removed. The agreement is best in the Bight, where simultaneous observations of surface winds and currents are used to derive the bottom resistance coefficient for the whole shelf. The resemblance between the two deteriorates away from the Bight stations, although general agreement remains except at Key West, where the bathymetry has been altered substantially.

Mitchum and Sturges' (1981) current-meter moorings were located offshore of Cedar Key during 24 February to 20 March, 1980. The low-passed longshore current records are compared (Fig. 16) with model results at two grid points that are reasonably close to the geographical location of the moorings. For the inshore mooring in 22 m of water, the model result at (18, 23) shows some qualitative resemblance. For the offshore mooring in 44 m of water, results from (16, 23) even show some quantitative agreement between the two. Note the high speed predicted by the model at the end of the hindcast period. There is little correspondence to this in the alongshore wind-stress field (Fig. 14). Model sea-level fields (not shown) show the formation of alternating regions of low and high sea level, as seen in the preliminary model experiments. The large y-directed velocity appears to be due to the formation of a sea-level low just outside the Bight that creates a south-to-north flow within the Bight. Evidence for the presence of propagating phenomena can again be sought from an examination of a y–t plot of sea level through the entire hindcast period (Fig. 17). Inshore at $i = 18$, the rapid response to winds is marked by a sea-level drop around day 6 when the cold front passed Tampa ($j = 18$), but, afterward, there is not the fast-moving shelf wave that was found for the case of the ideal front (Fig. 12). Free-wave propagation to the north following the passage of the cold front is evident in

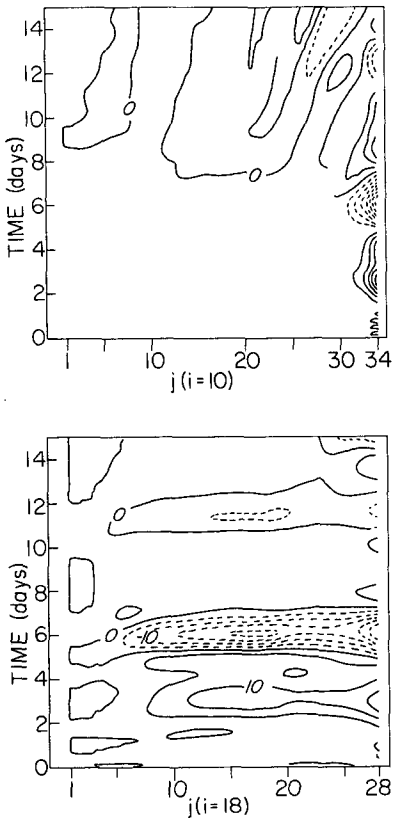

FIG. 17. Sea level contours in y–t space for the hindcast experiment: (top) i = 10, along the slope; (bottom) i = 18, on the shelf.

the y–t plot at i = 10 (offshore over the continental slope). There, toward the end of the hindcast period, slowly moving (at 25 km day^{-1} speed) waves appear to the north (j = 20–34). These waves contribute to the formation of sea-level lows and highs that may be ultimately responsible for the large alongshore velocity at (16, 23) that is unaccounted for in the wind-stress record.

6. Discussion

A significant result from the model studies has been the generation of mesoscale eddies along the shelf-slope junction that appears to occur when transports across the shelf break are forced by the wind-driven circulation on the shelf. Models that end with a zero-adjusted sea level at the shelf break miss this feature completely (e.g., Beardsley and Haidvogel, 1981). Cross-shelf transports at the break do apparently take place in the real world. Fig. 18 presents line-drawing representations of two VHRR images that support this contention. Fig. 18a shows an outflow of shelf water under a northerly surface wind field on 22 February 1981 following the passage of a cold front. Fig. 18b shows an onshore movement on 14 March 1978 of warm open ocean water during the first part of the hindcast period when the winds are southerly. These apparent cross-shelf-break movements appear to take place approximately where similar movements are suggested in the wind-driven model (Fig. 9). The correspondence is, at the surface, fortuitous since the model neglects the Loop Current and its eddies that are carriers of the observed high-surface-temperature signals. Can these lateral movements be forced by oceanic processes? Huthnance (1981) considered theoretically the transmission of oceanic Rossby waves across a vertical scarp and showed nearly total reflection at frequencies much less than the inertial frequency. More recently, Csanady and Shaw (1981) studied the bottom-pressure perturbation associated with steady flow over the continental slope in a heat-conduction analogy, and showed that the large bottom slope is equivalent to a large heat capacity that makes the slope region inert. Thus the shelf is effectively shielded from oceanic influences by the steepness of the continental slope. Large excursions of the boundary between the shelf and oceanic water masses may indeed owe their existence to the wind-driven circulation on the continental

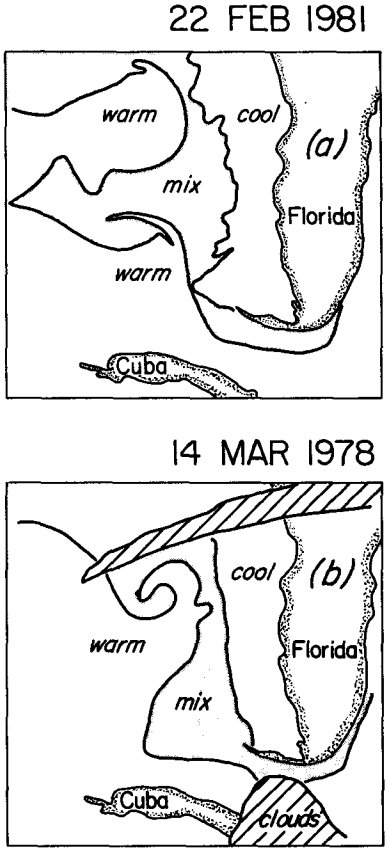

FIG. 18. Line drawing representation of VHRR images of SST contrasts over the eastern Gulf of Mexico. Shaded areas exhibit a mixture of warm and cool waters in patches. (a) NOAA 6 image on 22 February 1981, (b) NOAA 5 image on 14 March 1978.

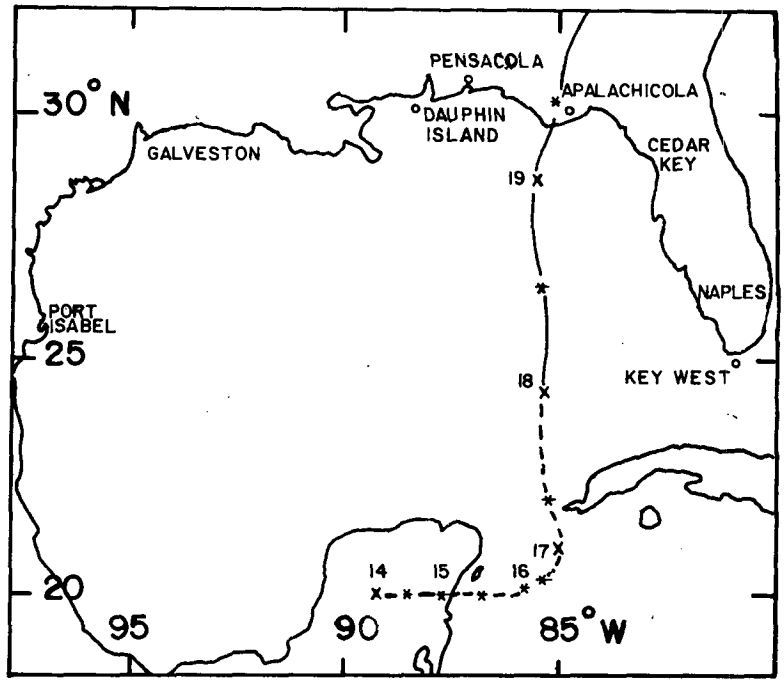

FIG. 19. The track of Hurricane Agnes through the Gulf of Mexico in June 1972. (from Ichiye, 1973). Dashed portion of the curve represents the path of the tropical storm before it became Hurricane Agnes. The crosses mark the position of the storm/hurricane at 0700 EST on the day dated with a two-digit number. The asterisks mark the storm/hurricane position at 1900 EST.

shelf. This would be in accord with the observed fact that, when temperature contrasts allow their detection from space, the Loop Current meanders occur mostly on the shelf side (Vukovich, personal communication). Eddy kinematics off the West Florida Shelf have been examined from direct current-meter records on the basis that they are Loop-Current driven (Niiler, 1976). Could it be that even these are also initiated by the cross-shelf-break flow mentioned here?

The appearance of slowly moving waves (upper panel, Fig. 17) during a period of relatively low winds following the passage of the cold front in the hindcast is of interest. It is suggestive of reflection of long waves. The phase of these slowly moving waves, as represented by lines of constant sea-level heights, propagates to the north, while the group appears to move southward, as indicated by the successive appearance of sea-level highs and lows in the upper right-hand corner of the y–t plot along $i = 10$. The reflection appears to be originating from the convergence of isobaths to the west (See Fig. 2). Hindcasts (not shown) with identical winds but parallel depth contours show little short-wave formation. Whatever wave reflection there might be from the imposition of a zero sea level at the open west end must have been small. Reflection of long waves at the Mississippi Delta has been observed at least once. During the passage along 85°W of Hurricane Agnes in June 1972, the highest sea level at Pensacola, Florida was reached at 1400 on June 19, approximately 9 h after the arrival of highest sea level at Dauphin Island, Alabama (Ichiye *et al.*, 1973). Hurricane Agnes, following a nearly south–north track through the Gulf of Mexico, struck land just west of Apalachicola, Florida shortly before 1900 that day. (See Fig. 19 for the track of Agnes and Fig. 20 for relevant sea-level records.)

7. Conclusions

Experimentation with a time-dependent, linearized, storm-surge model on the West Florida Continental Shelf has shown that:

1) Solutions to steady wind fields are coastally trapped with geostrophically balanced alongshore flow. For example, an e-folding scale measured offshore of Cedar Key is about 140 km (inshore of the 40 m isobath).

2) Adjustment to nearly steady patterns occurs in a time that appears to decrease from about a day in the northern part of the shelf to less than one-half day in the southern part.

3) Transient oscillations with periods of 11–15 h are excited by sudden turn-on of the wind.

4) Vorticity waves appear to be excited by cross-

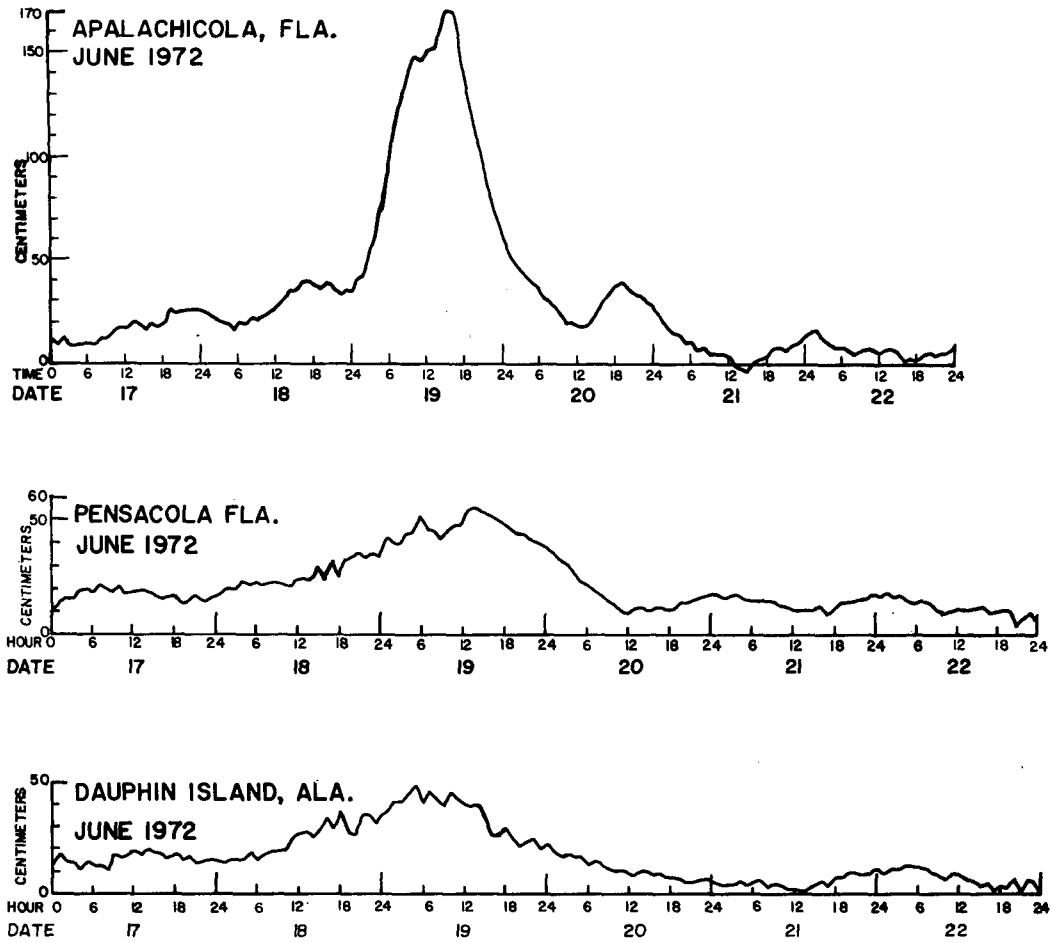

FIG. 20. Sea-level elevations at Apalachicola, and Pensacola, Florida and Dauphin Island, Alabama during the passage of Hurricane Agnes in June 1972. (From Ichiye, Han, Carnes, 1973.)

shelf-break wind-driven mass exchanges and give rise to 100 km sized geostrophic eddies that propagate along the continental slope at speeds of 25–100 km day^{-1}. Shelf waves with speeds on the order of 500 km day^{-1} have been found only in one, very idealized, case.

5) Modeled coastal sea level is in reasonable agreement with observed values over a 14-day hindcast period. Modeled currents are in qualitative agreement with actual mid-shelf currents during the time they were observed; beyond this time, when the wind forcing was relatively weak, large modeled currents associated with an eddy were dominant.

Acknowledgments. This research was supported by the National Science Foundation under Grant OCE80-15656 and the Office of Naval Research under Contract N00014-82-K-0082. The NOAA 6 image of the sea surface temperature contrast on 22 February 1981 and the NOAA 5 image of the same on 14 March 1978 are made available to the authors by Dr. Fred Vukovich of the Research Triangle Institute and Dr. Oscar Huh of the Louisiana State University, respectively. The manuscript was typed and figures drafted by Beverly Morris. The permission from Professor T. Ichiye for the use of two figures from the cited Texas A&M report is also acknowledged. Donna Arnold typed the revision and drafted Figs. 19 and 20.

REFERENCES

Beardsley, R. C., and D. B. Haidvogel, 1981: Model studies of the wind-driven transient circulation in the Middle Atlantic Bight. Part 1: Adiabatic boundary condition. *J. Phys. Oceanogr.*, **11**, 355–375.

Bowman, J. Malcolm, Alick C. Kibblewhite and David E. Ash, 1980: M_2 tidal effects in Greater Cook Strait, New Zealand. *J. Geophys. Res.*, **85**, 2728–2742.

Brown, W., W. Munk, F. Snodgrass, H. Mofjeld and B. Zetler, 1975: MODE bottom experiment. *J. Phys. Oceanogr.*, **5**, 75–85.

Cragg, J., G. T. Mitchum and W. Sturges, 1982: Wind-induced coastal currents and sea-surface slopes in the eastern Gulf of Mexico. Submitted to *J. Phys. Oceanogr.*

Csanady, G. T., 1978: The arrested topographic wave. *J. Phys. Oceanogr.*, **8,** 47–62.

—— and P. T. Shaw, 1981: Currents over the upper continental slope: Why are they so weak? *Trans. Amer. Geophys. Union,* **62,** p. 922 (Abstract).

Fernandez-Partagas, J., and C. N. K. Mooers, 1975: A subsynoptic study of winter cold fronts in Florida. *Mon. Wea. Rev.*, **103,** 742–744.

Gill, A. E., and E. H. Schumann, 1974: The generation of long shelf waves by the wind. *J. Phys. Oceanogr.*, **4,** 83–90.

Hsu, S. A., 1981: Models for estimating offshore winds from onshore meteorological measurements. *Bound.-Layer Meteor.*, **20,** 341–351.

Hsueh, Y., 1980: On the theory of deep flow in the Hudson Shelf Valley. *J. Geophys. Res.*, **85,** 4913–4918.

Huthnance, J. M., 1981: A note on baroclinic Rossby wave reflection at sea-floor scarps. *Deep-Sea Res.*, **28A,** 83–91.

Ichiye, Takashi, Han-Hsiung Kuo and Michael R. Carnes, 1973: Assessment of currents and hydrography of the eastern Gulf of Mexico. Tech. Rep., Dept. Oceanography, Texas A&M University.

Leendertse, J. J., 1967: Aspects of a computational model for long-period water wave propagation. The Rand Corporation, Santa Monica, RM-5294-PR, 165 pp.

Marmorino, George O., 1982: Wind-forced sea level variability along the West Florida Shelf (winter, 1978). *J. Phys. Oceanogr.*, **12,** 389–405.

Mitchum, Gary T., and W. Sturges, 1982: Wind-driven currents on the West Florida Shelf. *J. Phys. Oceanogr.*, **12** (in press).

Niiler, P. P., 1976: Observations of low-frequency currents on the West Florida continental shelf. *Mém. Soc. Roy. Sci. Liege,* 6th ser., **10,** 9–26.

Price, J. F., and C. N. K. Mooers, 1974: Shelf dynamics winter experiment, February-March 1973: Current meter data report. UM-RSMAS-74020, University of Miami, 78 pp.

Scott, J. T., and G. T. Csanady, 1976: Nearshore currents off Long Island. *J. Geophys. Res.*, **81,** 5401–5409.

Vansant, Linda, 1980: A numerical model of tidal currents in Apalachicola Bay, Florida. M. S. thesis, Dept. Oceanography, Florida State University, 85 pp.

Wilson, Basil W., 1972: Seiches. *Advances in Hydroscience,* Ven Te Chow, Ed., Vol. 8, Academic Press, 359 pp. (see pp. 1–94).